In Vivo Photocycle of the *Euglena gracilis* Photoreceptor

Laura Barsanti,* Vincenzo Passarelli,* Patricia L. Walne,# and Paolo Gualtieri*
*Istituto di Biofisica, CNR, I-56127 Pisa, Italy, and #Department of Botany, University of Tennessee, Knoxville, Tennessee 37996 USA

ABSTRACT We present the light-induced photocycle of the paraflagellar swelling of *Euglena gracilis*. The kinetics of this process was reconstructed by sampling its fluorescence emission and switching the excitation light from 365 nm to 436 nm. Stable intermediates in the photocycle were manifested. The measured millisecond resolution kinetics best fits a Michaelis-Menten equation. The data provide strong evidence that the paraflagellar swelling, a three-dimensional natural crystal of a light-detecting protein, is the true *Euglena* photoreceptor.

INTRODUCTION

Since the turn of the century the photosynthetic and photosensitive flagellate *Euglena* has provided an intriguing subject for photobiological studies. This flagellate dwells in natural shallow ponds, and uses sunlight as source of energy and information. Its chloroplasts are the energy-supplying devices, whereas a simple but sophisticated system is used as a light detector. Two flagella are inserted in a subapical invagination of the cell termed the reservoir. The stigma, composed of red-orange pigment granules, lies in the adjacent cytoplasm. Only one flagellum emerges from the cell and consists of an axoneme, a paraxial rod running parallel to it, and a swelling (paraflagellar body) near its base (Rosati et al., 1991). In fact the swelling, a three-dimensional natural crystal whose dimensions are about 1 μm $\times$ 0.7 μm $\times$ 0.7 μm, can be considered the first ciliary photoreceptor (Walne and Gualtieri, 1994). According to Eakin's theory (1968, 1972) the photoreceptor ciliary line of evolution, which had its climax in the elaborate and remarkably complex vertebrate photoreceptor, originated from this organelle.

As the cell rotates while swimming, the stigma comes between the light source and the paraflagellar swelling, thus modulating the light that reaches it, and regulating the steering of the locomotory flagellum (Jennings, 1906). This configuration of stigma, swelling, and flagellum can be considered a simple but complete visual system. The frequency of the rotation is 2 Hz (Ascoli et al., 1978).

The three-dimensional paraflagellar swelling, a proteic crystal (Gualtieri, 1993), can be interpreted as a 3D crystal of type I (Michel, 1990), i.e., a stack of 2D crystal arrays characterized by in-plane hydrophobic interactions and held together by hydrophilic interactions. On the basis of optical diffraction studies conducted on thin sections of the *Euglena* paraflagellar swelling, Piccinni and Mammi (1978) measured its crystalline monoclinic cell unit, the dimensions of which are a = 8.9 nm, b = 7.7 nm, c = 8.3 nm, β = 110°.

Other examples of naturally occurring crystalline light-detecting organelles are the 2D arrays of bacteriorhodopsin in the plasma membrane of *Halobacterium halobium*; the 2D arrays of large membrane particles forming the reaction centers of photosystem II in the photosynthetic membranes of green plants; and the photosynthetic membranes of *Rhodopseudomonas viridis* and related purple bacteria (Kuhlbrandt, 1992). Among these, the paraflagellar swelling of *Euglena* acquires a special meaning because it is the only crystal of a photodetecting protein consisting of about 100 layers (Gualtieri, 1993). Recent experimental results have suggested that it uses a rhodopsin-based detecting system.

In 1989 Gualtieri and co-workers (Gualtieri et al., 1989) and subsequently in 1992 Crescitelli and co-workers (James et al., 1992) measured the absorption spectrum of a single *Euglena* paraflagellar swelling. Because of the great similarity between these spectra and the absorption curve of the rhodopsin α-band centered at 500 nm, both research groups suggested a pigment such as the rhodopsin-like protein in the photosystem of *Euglena*. Successive experiments on inhibition of the swelling formation (Barsanti et al., 1992) and the extraction of retinal from intact and demembranated cells (Gualtieri et al., 1992, and successive developments; Barsanti et al., 1993) have provided data to further support the rhodopsin-like protein hypothesis.

However, the possible photoreceptive roles of the cytoplasmic stigma and the paraflagellar swelling of *E. gracilis* are still under debate, because of conflicting interpretations of the results produced so far by the different research groups working on this microorganism. In addition to rhodopsin, flavins and pterins have been suggested as photoreceptive pigments in *Euglena* (Schmidt et al., 1990; Brodhun and Häder, 1990), but their presence has been detected only in isolated flagella and not in the swelling (Galland et al., 1990; Sineshchekov et al., 1994). Recently, Neumann and Hertel (1994) purified a riboflavin-binding protein from isolated flagella of *Euglena gracilis* and documented the presence of these binding proteins in the entire flagellar membrane and not in the paraflagellar swelling.

Received for publication 29 July 1996 and in final form 13 November 1996.
Address reprint requests to Dr. Paolo Gualtieri, CNR Istituto di Biofisica, Via San Lorenzo, 26, I-56127 Pisa, Italy. Tel.: +39-50-513111; Fax: +39-50-553501; E-mail: mbxgualtieri@mail.cnuce.cnr.it.

0006-3495/97/02/545/09 $2.00

As a rule, prokaryotic and eukaryotic light-sensory proteins are capable of a cyclic photoregeneration, with identified intermediates. Selected examples of these proteins are the *Halobacterium* sensory rhodopsins (Marwan and Oesterhelt, 1990; Bogomolni and Spudich, 1991); the squid rhodopsin (Hubbard and St. George, 1958); the fly rhodopsin (Hamdorf and Schwemer, 1975); and the human rhodopsin as well, which has the possibility of photoreversal, but is commonly regenerated from separated components (Knowles and Dartnall, 1977).

In the case of *Euglena*, to positively identify the true photoreceptor, it is necessary to verify which endocellular compartment undergoes structural reversible changes upon illumination, to localize the photochromic proteins. Assuming the paraflagellar swelling to be a light-sensing device, it should show this characteristic, i.e., a cyclic photoreaction.

Because of the presence of a clearly detectable emission in the *Euglena* paraflagellar swelling, we decided to investigate its photobehavior by analyzing changes in the in vivo fluorescence. Although it is not possible to measure the λ_{max} of the new light-induced intermediates, these changes provide important information on the series of structural changes that *Euglena* photoprotein undergoes in response to light.

MATERIALS AND METHODS

Cultures

Cultures of *Euglena gracilis* strain Z cells (Sammlung von Algen Kulturen, Göttingen, 1224-5/25) were grown axenically in autotrophic Cramer-Myers medium (0.025 M) in sodium acetate (pH 6.8) (Cramer and Myers, 1952), under constant temperature (24°C) and continuous illumination (500 lux).

Demembranation

The demembranating solution was prepared as follows. Triton X-100 was dissolved in a HEPES-buffered solution (100 mM HEPES-KOH, pH 7.00; 20 mM piperazine-N,N′-bis(2-ethanesulfonic acid); 10 mM EDTA; 50 mM sucrose; 1 mM dithiothreitol; 7.5% v/v glycerol) to a final detergent concentration of 4% v/v, filtered, and added to the cells (4:1), which were previously suspended in 100 mM HEPES buffer (pH 7.00). Cells were incubated overnight at room temperature and then washed twice with HEPES buffer to remove the extracted chlorophyll.

Hardware

The hardware platform consists of a Zeiss Axioplan fluorescence microscope (Zeiss, Oberkoehen, Germany) equipped with an epifluorescence system, a 100× (N.A. 1.3) and a 20× (N.A. 0.5) planapochromatic objective, a 100-W mercury lamp, and a monochrome CCD camera (NXA 1011/01; CCIR Standard, Philips, Netherlands), which ensures geometric accuracy, stability, linearity, and sensitivity. The video signal is used as the input for the image system board (FG100AT; Image Technology), which is plugged into the bus of a personal computer (IBM). The board consists of a frame memory (1024 × 1024 × 12 bit), a multiplexer, a 4096 × 12 bit feedback input look-up table (LUT), and an A/D converter. The multiplexer has 24 input bits: 12 from frame memory, 8 from the A/D converter, and 4 from the LUT control register. The A/D converter samples the analog video signal of the TV camera at 12.5 MHz. According to the CCIR standard the size of the digitized image is 640 × 512 × 8 bits, with equal vertical and horizontal spacing. A black and white monitor (BM 7542; Philips, Netherlands) is used to display the signal output of the TV camera, and an RGB high-persistence monitor (C-3479; Mitsubishi, Tokyo, Japan) is used to display the digital image.

Fluorescence microscopy

Fluorescence images from *Euglena* cells were acquired with the following filter combinations: a UV-blue set (8-nm band-pass excitation filter, 365 nm; chromatic beam splitter, 395 nm; barrier filter, 397 nm; 800 $\mu W/cm^2$) and a blue-violet set (8-nm band-pass excitation filter, 436 nm; chromatic beam splitter, 460 nm; barrier filter, 470 nm; 1100 $\mu W/cm^2$). Because of the spectral distribution of the high-pressure mercury lamp, these two excitation wavelengths are the only two available for our measurements, because any other excitation wavelength has a fluence rate lower than 50 $\mu W/cm^2$, and the induced photomodifications, if any, are below the detection limits of our visual and acquisition system. In only one experiment a 50-W high-pressure xenon lamp was used in combination with a wide-band blue-violet set (400–440-nm wide-band excitation filter; chromatic beam splitter, 460 nm; barrier filter, 470 nm; 800 $\mu W/cm^2$). Irradiances were measured with a hand-held optical power meter (model 840; Newport). In this particular case UV absorption microspectrophotometry proved to be less useful than fluorescence microspectrophotometry for both the very sophisticated instrumental set-up necessary for such a measurement and the intrinsic fluorescence characteristics (Gualtieri, 1991).

Software

Fluorescence images were acquired and digitized every 40 ms. Each digitized image, consisting of 320 × 200 pixels, represents the apical part of the cell, where the paraflagellar swelling is located. Fifteen images for each excitation wavelength were stored in the frame memory. Because of our hardware facilities, the operations of panning, scrolling, and storing were performed during the frame acquisition (Gualtieri and Coltelli, 1991). Digital image techniques such as segmentation and labelization procedures were applied to each fluorescence image to automatically select and measure the integrated emission of the *Euglena* paraflagellar swelling (Coltelli and Gualtieri, 1990). The resulting variation versus time was plotted and analytically fitted using the Sigma Plot package (Jendel).

Photography

Fluorescence, bright-field, and phase-contrast photographs were taken with a Minolta X-100 camera mounted on a Zeiss Axioplan microscope, and recorded on Kodak Ektachrome 100 ASA color film.

RESULTS

The changes in fluorescence of the paraflagellar swelling of *Euglena gracilis*, in response to two different excitation lights (436 nm and 365 nm) are shown in Figs. 1 and 2. The 436-nm excitation light (blue-violet filter set) produces the typical red fluorescence of chloroplasts, and faint or no fluorescence in the paraflagellar swelling zone (Figs. 1 *a* and 2, *a* and *c*). Fig. 2 *b* shows the effect of a prolonged exposure (5 min) to the 436-nm light: apart from chlorophyll bleaching, no detectable modification of the swelling's emission can be observed. Under the 365-nm excitation light (UV-blue filter set), the paraflagellar swelling undergoes an increase in its emission from zero (Fig. 1 *b*) to a maximum (Fig. 2 *d*) in the green range. With the blue-

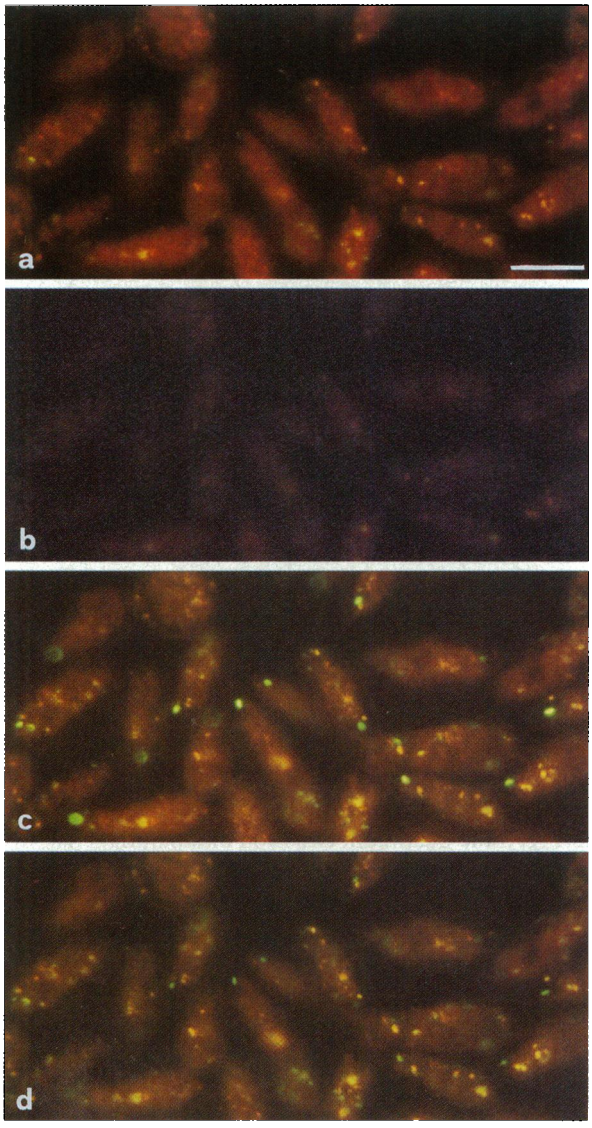

FIGURE 1 Fluorescence micrographs of *Euglena gracilis* cells at low magnification (20×). Under the 436-nm excitation light the cells show the typical red emission of the chlorophyll, and faint or no emission in the paraflagellar swelling area (*a*). The 365-nm excitation light produces an increase in the emission of the swelling from zero (*b*) to a maximum in the green range. Under the 436-nm excitation light this emission appears extremely bright (*c*) and then fades (*d*). Scale bar = 50 μm.

violet filter inserted, the swellings now appear as bright green bodies (Figs. 1 *c* and 2 *e*), whose emission gradually fades (Figs. 1 *d* and 2 *f*). Visual observations do not detect any chromatic difference in the emission hue of the swelling under the two excitation lights. Moreover, the insertion of dark periods during and between excitations does not modify the fluorescence intensity attained.

To reconstruct the kinetics of this photocycle we sampled the fluorescence emission of the paraflagellar swelling, digitizing at constant rate fluorescence images of 20 *Euglena* cells. Two sequences were created, one for the UV-blue excitation light and the other for the blue-violet excitation light. Fig. 3 shows these two sequences of 15 320 × 200

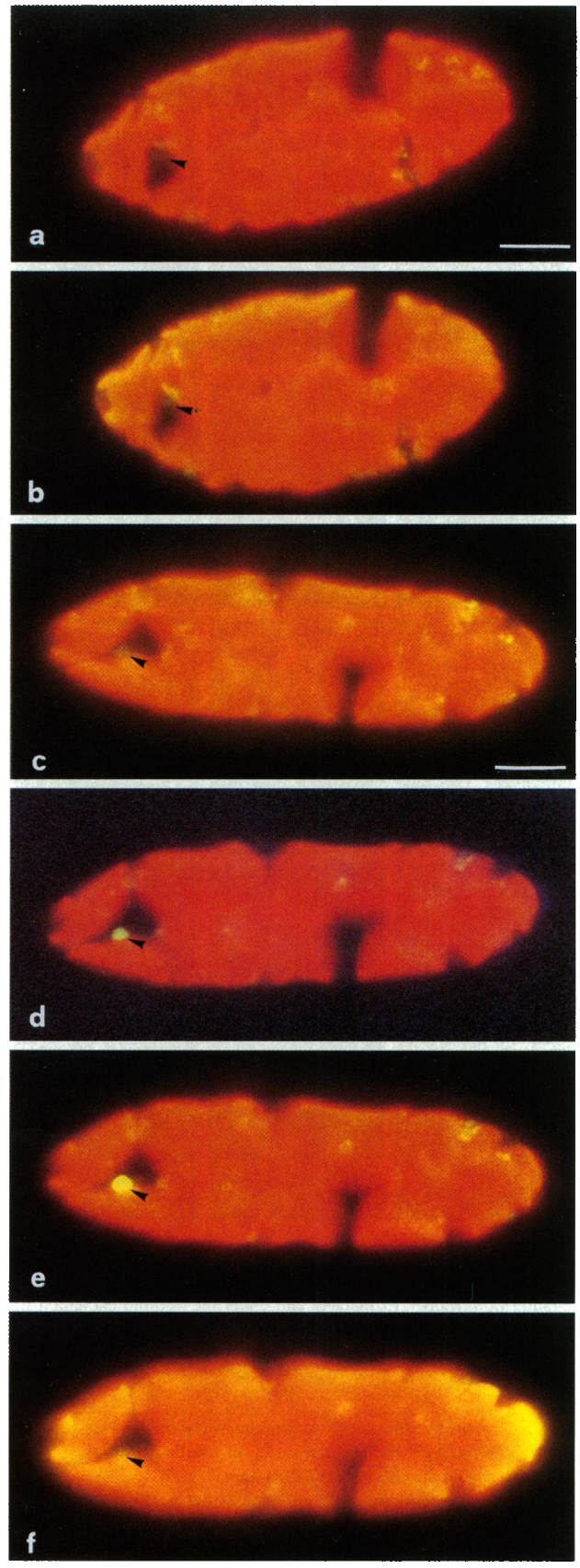

FIGURE 2 Fluorescence micrographs of *Euglena* cells at high magnification (100×). (*a* and *b*) The same cell under the 436-nm excitation light:only a very faint emission is detectable in the paraflagellar swelling area

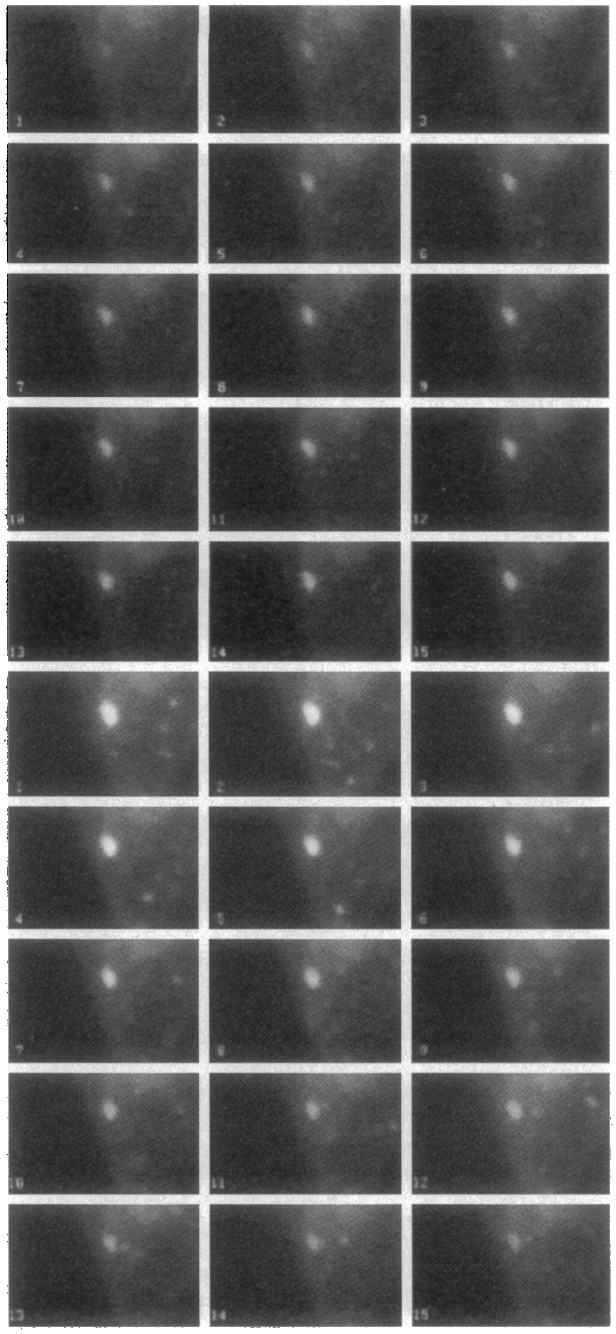

FIGURE 3 Two sequences of black-and-white digitized fluorescence images show the variation of the emission of a swelling under the 365-nm excitation light (upper 15 images) and under the 436-nm excitation light (lower 15 images). Each image represents the apical part of a cell, where the paraflagellar swelling is located.

(*a*), and a prolonged exposure (5 min) to this wavelength produces bleaching of the chlorophyll, but no increase in the swelling's emission (*b*). (*c*) Another cell under the 436-nm excitation light. The 365-nm excitation light produces an increase in the green emission of the swelling from zero (cf. Fig. 1 *b*) to a maximum in the green range (*d*). Under the 436-nm excitation light (*e*) this bright emission gradually fades (*f*). The bright green appearance of the microscopic image of the swelling becomes yellowish-green (*e*) because of a local overexposure of the photographic film due to the high intensity of the swelling's emission. In all of the figures the arrowheads point to the swelling. Scale bar = 10 μm.

pixel digital fluorescence images. The 30 black-and-white digitized images represent the apical part of the same *Euglena* cell, where the swelling is located. The upper 15 images, acquired every 400 ms (10 TV frames), show the swelling emission under the 365-nm excitation light, whereas the lower 15 images, acquired every 640 ms (16 TV frames), show the emission under the 436-nm excitation light. From the top left corner to the bottom right corner the successive images show the variation of the emission from the lowest intensity to the highest and vice versa.

Segmentation and labelization techniques were applied to each of the 30 digital fluorescence images. These procedures select all of the pixels belonging to the swelling in the apical region of *Euglena*, count them, and add up their intensity values. The resulting values represent the integrated emission of the swelling. The variation of these values versus time was plotted after an analytical fit. This kinetics clearly indicates the presence of a complex chain photoreaction with at least three intermediates (Fig. 4). A represents the parent form of the protein; B (and/or B′) and C (and/or C′) are the two light-induced intermediates, which revert to A at the end of the cycle. The formation of each intermediate best fits with a Michaelis-Menten equation of form $ax/(x + b)$ ($\chi < 1$). Fig. 4 shows the fitted kinetics in its upper part and the distribution of residues between the row and the fitted data in its lower part.

In Fig. 5 the maximum emission of a paraflagellar swelling (Fig. 5 *a*) is compared with the emission of a swelling

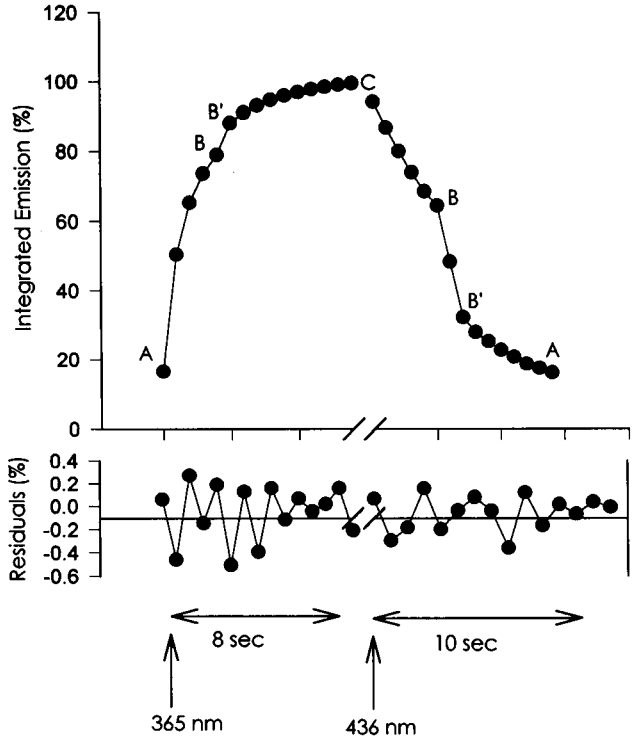

FIGURE 4 Kinetics of the photocycle of the swelling indicates the presence of at least three forms, i.e., A, B, and C. The distribution of residues between the row and the fitted data is shown in the lower part of the figure.

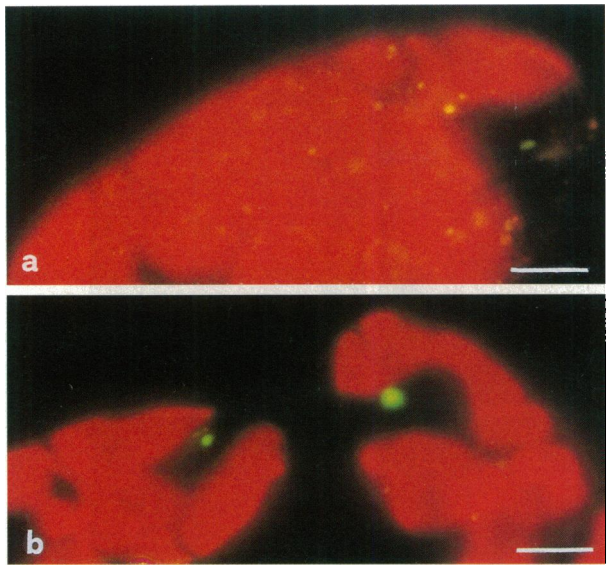

FIGURE 5 The emission of a flagellar swelling under a 400–440-nm wide-band excitation light (i.e., simultaneously with the UV and the blue excitations; *a*) is compared with the emission under the 436-nm light of a swelling previously excited with the 365-nm light (*b*). The difference is impressive. Scale bar = 10 μm.

excited with a 400–440-nm wide-band filter (i.e., simultaneously with the UV and the blue excitation wavelengths) (Fig. 5 *b*).

Repeated cycles can be observed in living cells, but under prolonged microscopic observation the slides dry up and the cells burst. This fact prevents the recording of many consecutive cycles in the same cell. To make the cells more resistant to dehydration, we treated them with a detergent solution that effects complete extraction, with the exception of pellicle, axonemes, the paraflagellar rod, the paraflagellar swelling, and the microtubular system of the reservoir-canal region (refer also to figures 8–10 in Barsanti et al., 1993). Three successive photocycles of the same swelling are shown in Fig. 6; the bright-field and phase-contrast images show the swelling as a gray or dark body, respectively (Fig. 6, *a* and *b*, *arrowhead*); its fluorescent image under the 436-nm light shows only a faint emission (Fig. 6 *c*), which increases to a maximum under the 365-nm light (Fig. 6, *d*, *h*, *l*). Under the 436-nm excitation light this emission appears extremely bright (Fig. 6, *e*, *i*, *m*) and then gradually fades (Fig. 6, *f*, *g*, *j*, *k*, *n–p*). Because of the almost complete extraction of pigments, the 365-nm irradiation produces a different cellular hue (Fig. 6, *d*, *h*, *l*). The same intensity and same time of irradiation at 365 nm (800 μW/cm^2) and 436 nm (1100 μW/cm^2) were obviously adopted throughout the three cycles.

This photocycle would thus include the photoconversion under the 365-nm excitation light of a nonfluorescent form (A) to two or more fluorescent intermediates, which remain stable almost indefinitely (C); these in turn would regenerate the nonfluorescent form under the 436-nm excitation light.

DISCUSSION

We report the presence of a photochromic pigment in the paraflagellar swelling of *Euglena gracilis* that undergoes repeated and reversible fluorescence changes with a determinate kinetics; this cycle is present not only in cells under physiological conditions, but also in cells treated with a detergent solution that completely extracts them (Fig. 6). The paraflagellar swelling possesses optical bistability, i.e., the parent form of its molecules upon photoexcitation generates relatively stable intermediate(s) that can be photochemically driven back to the parent form, and the quantum yields of the forward and reverse reactions are almost the same (Fig. 4). The A form is not fluorescent.

These data allow us to identify the true photoreceptor of *Euglena gracilis* with its crystalline paraflagellar swelling, and seem to us to support the hypothesis of a rhodopsin-based photoreceptor.

Photochromism with nearly similar forward and reverse reaction quantum yields, both close to unity, is peculiar to rhodopsins (Govindjee et al., 1990; Marwan and Oesterhelt, 1990; Siebert, 1990; Birge et al., 1995). Stable intermediates are very often present in the photocycle of rhodopsins, particularly in invertebrate rhodopsins (Hamdorf and Schwemer, 1975; Franceschini, 1983); and the bacteriorhodopsin itself offers a good example of a cycle with thermally stable intermediates whose lifetime can be relatively easily modified (Birge, 1995; Birge et al., 1995).

Data already cited provide an estimate of 2×10^7 molecules of rhodopsin-like proteins in the crystalline structure of the paraflagellar swelling of *Euglena gracilis* (Gualtieri et al., 1989, 1992). Considering that in the present experiment about 10^8 photons impinge on the swelling area and produce a saturation effect (maximum number of stable intermediate(s)) and assuming that the *Euglena* photoreceptor operates via a one-photon absorption mechanism, we can approximate the forward and reverse quantum yields of its cycle kinetics to unity, as expected.

Having stated this, we can describe the cycle we recorded in *Euglena gracilis* in the following way. The initial form A, present in a very high percentage in this state of photoequilibrium, has a very low absorbance at 436 nm and a higher absorbance at 365 nm, and does not fluoresce. It could resemble the resting state of a rhodopsin-like protein with an α-band at 500 nm and a secondary β-band centered in the UV-blue region (Stavenga et al., 1993), as suggested by Gualtieri et al. (1989) and James et al. (1992).

The intermediates, B and C, emit in the green range; we cannot visually detect any difference in the emission hue of the paraflagellar swelling under the two excitation lights. Because they produce a green emission, these intermediates should have an absorption band bathochromically shifted in comparison with the parent A, and absorb the incident light at 365 nm and at 436 nm, respectively. Either a change in the polarity of the binding pocket or the intrinsic constraints of their excited state, both due to proteic and/or chromophoric conformational changes, can enhance their quan-

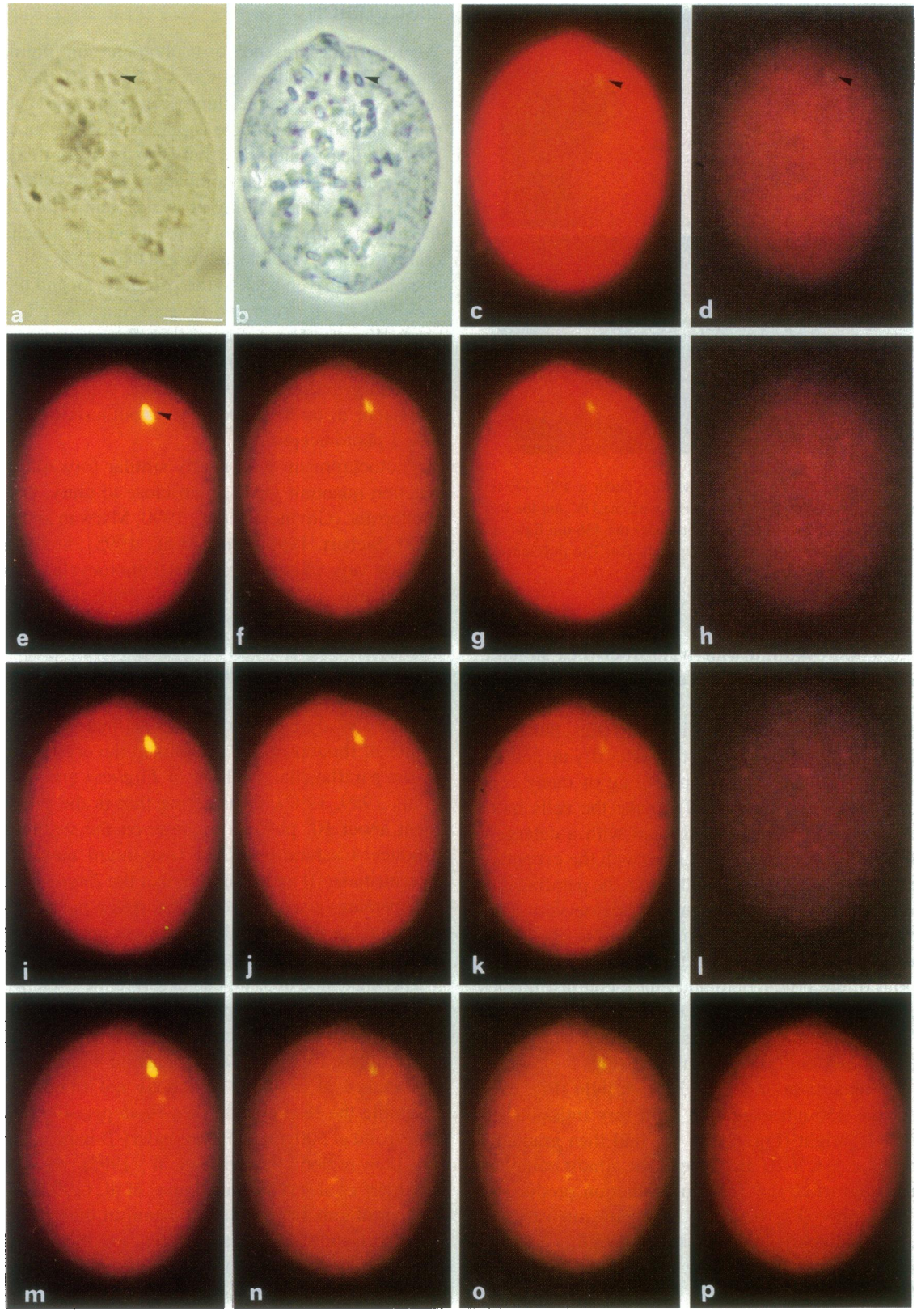

FIGURE 6 Three photocycles of the same demembranated cell are shown. In bright-field (*a*) and in phase-contrast (*b*) images, the paraflagellar swelling is visible as a gray or dark body, respectively. Under the 436-nm excitation light, its emission is very faint (*c*), but under the 365-nm light increases from zero (*d, h, l*) to a maximum. Under the 436-nm excitation light this emission appears extremely bright (*e, i, m*) and then gradually fades (*f, g, j, k, n–p*). Because of the almost complete extraction of pigments, the 365-nm excitation light produces a different hue in the cell (*d, h, l*). As in Fig. 2 *e*, the bright green appearance of the microscopic image of the swelling becomes yellowish because of a local overexposure of the photographic film due to the high intensity of the swelling's emission. In all of the figures the arrowhead points to the swelling. Scale bar = 10 μm.

tum yields. The photoinduced rhodopsin-like intermediates such as metarhodopsin I and metarhodopsin II have these spectroscopic characteristics. These two new species, meta I and meta II, are structurally related and are in a pH-sensitive equilibrium. In invertebrates such as squid, cuttlefish, octopus, and insects, in which the sequence of the intermediates ends with these two thermostable species (meta I and meta II), the protonated form has its λ_{max} in the blue region and the neutral form has its λ_{max} in the near-UV region. As already shown (Goldsmith, 1972), blue-light irradiation reconverts these intermediates to the parent form, i.e., all metarhodopsins to rhodopsin. The in vivo fluorescence behavior of fly rhabdomeres was investigated by Franceschini and co-workers (Franceschini et al., 1981; Franceschini, 1983); when excited with UV or blue lights these photoreceptors emit throughout the entire visible range, from green to red. In vertebrates, where bleaching occurs, metarhodopsin I, the neutral form, has its λ_{max} bathochromically shifted in comparison with the parent pigment; metarhodopsin II, the protonated form, has the λ_{max} that lies in the near-UV region (Knowles and Dartnall, 1977). The fluorescence emission of these last two forms, meta I and II, was investigated by Guzzo and Pool (1968, 1969) at low temperatures in cattle rod outer segments and in cattle rhodopsin-digitonin micelles. Digitonin micelles emitted in the 510–560-nm range, whereas the dry rod outer segment emitted in the 530–580-nm range (in both cases 400-nm and 440-nm excitation wavelengths were used). With this description in mind, we could suggest acid and alkaline metarhodopsins as the B and C intermediates of the *Euglena* photocycle. In fact, our proposed photosystem is similar to that of the cephalopod *Eledone* (Schlecht and Tauber, 1975), for example, except that its thermostable acid metarhodopsin is shifted to longer wavelengths in comparison to *Euglena*.

Using both the 365-nm and the 436-nm excitation lights to irradiate the photoreceptor, we should expect a photoequilibrium among the nonfluorescent A form, and the fluorescent B and C intermediates; therefore, the emission intensity of the photoreceptor can vary from a maximum intensity (saturation) to zero, depending on the ratio of the two excitation lights. With our setup, we cannot irradiate simultaneously with both the 436-nm and the 365-nm excitation lights. As an approximation, we can acquire a fluorescence image of *Euglena* by using a 50-W xenon lamp with a 400–440-nm wide-band excitation filter. As expected, the emission of the paraflagellar swelling excited with this wide-band filter is faint (Fig. 5 *a*) in comparison with the emission of the swelling at maximum fluorescence intensity (Fig. 5 *b*).

The analogy between the photocycle kinetics and the Michaelis-Menten equation for enzyme kinetics allows us to hypothesize that the sensory protein we identified as a rhodopsin-like protein behaves like an enzymatic substrate, i.e., it reacts with light to form a photoactivated enzyme-substrate complex, which in this case would be represented by the activated intermediates B and C. These intermediates could be responsible for *Euglena* photobehavior. The other two intermediates, B′ and C′, could also be photoinduced, but on the basis of our data, we can provide no explanation at present.

Characteristics, such as emission maxima, fluorescence quantum yields, and thermal intermediate lifetime, of rhodopsin-like proteins are known to strongly depend on many factors. In vertebrates, rhodopsin embedded in the intact rod and in the digitonin micelle are known to possess different fluorescence spectra because of their different chemical environments (Guzzo and Pool, 1969); in invertebrates, such as flies, the optical bistability of the rhabdomere is related to the crystalline structure of this organelle (Franceschini, 1983). In halobacteria, the thermal transition between the intermediates M and bR of bacteriorhodopsin is susceptible to temperature, genetic modification, chromophore substitution, and chemical environment (Birge et al., 1995). For our photoreceptor, we can postulate that the spectroscopic characteristics of B and C intermediates are influenced by the limited flexibility of the protein in the 3D crystalline structure of the photoreceptor of *Euglena*. The crystal lattice could either force the protein to assume only a few of the possible conformational states, or actually induce a novel conformational structure (Gabellieri et al., 1988). These constraints could also explain the possible slow kinetics of the formation of the intermediates in comparison with all of the other measured photocycles (Bogomolni and Spudich, 1991).

For the sake of clarity, we would like to compare our findings with the flavin-pterin hypothesis.

We reported that the photochromic parent form A of the protein present in the swelling and not in the flagellar membrane is not fluorescent, either under 436-nm light or under 365-nm light (Fig. 1, *a* and *b*), thus excluding the presence of fluorescent species such as pterins and flavins in this organelle.

Changes in fluorescence intensity recorded on flagellar suspensions were reported by Sineshchekov et al. (1994) and by Neumann and Hertel (1994). According to these authors, those changes in the blue region of the spectrum that are only visible on maltreated flagellar material are produced by a greater fluence rate (2 W/m^2) and after an irradiation time of almost 3 h. Moreover, because of the stress placed on the samples, these changes are not reversible.

Light-induced absorption changes (LIACs) are photoresponses induced by intense blue irradiation (Lipson and Horowitz, 1991). They have been reported, for example, in *Phycomyces* (Lipson and Presti, 1977), *Neurospora* (Muoz and Butler, 1975), *Dictyostelium* (Poff and Butler, 1974), and *Trichoderma* (Horwitz et al., 1986). Data obtained from extracts of *Phycomyces* sporangiophores can be used as an example of relatively empirical LIACs (Trad et al., 1988). In this work, the researchers recorded a small absorbance change after an initial blue irradiation and a larger change of opposite sign induced by UV irradiation when UV light was given either as the first irradiation or after the blue. In this

experiment, an irradiation program different from the one we used was applied, i.e. blue light, UV-A light, and blue light again, with a 5-min interval between successive irradiations. The reported kinetics had a different time scale (minutes), with different quantum yields, presumably low for the forward and for the reverse reactions; this latter reaction was not completed. The blue and the UV-A fluence rates were, respectively, 560 W/m^2 and 93 W/m^2, which are higher that the ones we used.

LIACs typically show an absorption increase at 427 nm and an absorption decrease near 450 nm. It is generally assumed that the oxidized flavin is photochemically reduced by an unknown electron donor, thus creating an absorbance decrease at 450 nm, the absorption maximum of flavins. The reduced flavin would in turn transfer an electron to the *b*-type cytochrome, and increase its absorption peak at 427 nm. Therefore, if the paraflagellar swelling of *Euglena* were to undergo LIACs, we should observe a decrease in the fluorescence emission for the reduction followed by an emission increase at the reoxidation. But we recorded the completely opposite phenomenon. Moreover, because we can record many successive photochromic cycles on the same swelling, in our opinion such a complex mechanism (reduction and oxidation reactions, compulsory presence of electron donors and acceptors) is unlikely to be present in a photoreceptor with a crystalline structure that has been deprived of all the necessary biochemical pathways (Fig. 6). All of these differences make difficult the comparison between these data and our results.

In our opinion, flavins and pterins are present in the flagellar membrane of *Euglena*, but their function is probably not related to the photochromism of the photoreceptor.

REFERENCES

Ascoli, C., M. Barbi, C. Frediani, and A. Mure. 1978. Measurements of *Euglena* motion parameters by laser light scattering. *Biophys. J.* 24: 585–599.

Barsanti, L., V. Passarelli, P. Lenzi, and P. Gualtieri. 1992. Elimination of photoreceptor (paraflagellar swelling) and the photoreception in Euglena *gracilis* by means of the carotenoid biosynthesis inhibitor nicotine. *J. Photochem. Photobiol.* 13:135–144.

Barsanti, L., V. Passarelli, P. Lenzi, P. L. Walne, J. R. Dunlap, and P. Gualtieri. 1993. Effects of hydroxylamine, digitonin and Triton X-100 on photoreceptor (paraflagellar swelling) and photoreception of *Euglena gracilis*. *Vision Res.* 33:2043–2050.

Birge, R. R. 1995. Protein-based computers. *Sci. Am. 272*, 90–95.

Birge, R. R., Z. Chen, D. Govender, R. B. Gross, S. B. Hom, K. C. Izgi, J. A. Stuart, J. R. Tallent, and B. W. Vought. 1995. Biomolecular photonics based on bacteriorhodopsin. *In* CRC Handbook of Organic Photochemistry and Photobiology. W. M. Horspool and P.-S. Song, editors. CRC Press, Boca Raton, FL. 1568–1586.

Bogomolni, R. A., and J. L. Spudich. 1991. Archaebacterial rhododpsins: sensory and energy transducing membrane proteins. *In* Sensory Receptors and Signal Transduction. J. L. Spudich and B. H. Satir, editors. Wiley-Liss, New York. 233–255.

Brodhun, B., and D.-P. Häder. 1990. Photoreceptor proteins and pigments in the paraflagellar body of the flagellate *Euglena gracilis*. *Photochem. Photobiol.* 52:865–871.

Coltelli, P., and P. Gualtieri. 1990. A procedure for the extraction of object features in microscope images. *J. Biomed. Comput.* 25:169–176.

Cramer, M., and J. Myers. 1952. Growth and photosynthetic characteristics of Euglena gracilis. *Arch. Mikrobiol.* 17:384–402.

Eakin, M. E. 1968. Evolution of photoreceptors. *Evol. Biol.* 2:194–240.

Eakin, M. E. 1972. Structure of invertebrate photoreceptors. *In* Handbook of Sensory Physiology, Vol. VII/1, Photochemistry of Vision. H. J. A. Dartnall, editor. Springer, Heidelberg. 625–684.

Franceschini, N. 1983. In-vivo microspectrofluorimetry of visual pigments. *In* The Biology of Photoreception. D. J. Cosens and D. Vince-Price, editors. Society for Experimental Biology, London. 53–85.

Franceschini, N., K. Kirschfeld, and B. Minke. 1981. Fluorescence of photoreceptor cells observed in vivo. *Science.* 213:1264–1267.

Gabellieri, E., G. B. Strambini, and P. Gualtieri. 1988. Tryptophan phosphorescence and the conformation of liver alcohol dehydrogenase in solution and in the crystalline state. *Biophys. Chem.* 30:61–67.

Galland, P., P. Keiner, D. Dörnemann, H. Senger, B. Brodhun, and D.-P. Häder. 1990. Pterin- and flavin-like fluorescence associated with isolated flagella of *Euglena gracilis*. *Photochem. Photobiol.* 51:675–680.

Goldsmith, T. H. 1972. The natural history of invertebrate visual pigment. *In* Handbook of Sensory Physiology, Vol. VII/1, Photochemistry of Vision. H. J. A. Dartnall, editor. Springer, Heidelberg. 685–720.

Govindjee R., S. P. Balashov, and T. G. Ebrey. 1990. Quantum efficiency of the photochemical cycle of bacteriorhodopsin. *Biophys. J.* 58: 597–608.

Gualtieri, P. 1991. Microspectrophotometry of photoreceptor pigment in flagellated algae. *Crit. Rev. Plant Sci.* 9:475–495.

Gualtieri, P. 1993. Euglena gracilis: is the photoreception enigma solved? *J. Photochem. Photobiol. B Biol.* 19:3–14.

Gualtieri, P., L. Barsanti, and V. Passarelli. 1989. Absorption spectrum of a single isolated paraflagellar swelling of *Euglena gracilis*. *Biochim. Biophys. Acta.* 993:293–296.

Gualtieri, P., and P. Coltelli. 1991. An automated system for the analysis of moving images. *J. Comput. Assist. Microsc.* 3:15–21.

Gualtieri, P., P. Pelosi, V. Passarelli, and L. Barsanti. 1992. Identification of a rhodopsin photoreceptor in *Euglena gracilis*. *Biochim. Biophys. Acta.* 1117:55–59.

Guzzo, A. V., and G. L. Pool. 1968. Visual pigment fluorescence. *Science.* 159:312–314.

Guzzo, A. V., and G. L. Pool. 1969. Fluorescence spectra of the intermediates of rhodopsin bleaching. *Photochem. Photobiol.* 9:565–570.

Hamdorf, K., and J. Schwemer. 1975. Photoregeneration and the adaptation process in insect photoreceptors. *In* Photoreceptor Optics. A. W. Snyder and R. Menzel, editors. Springer-Verlag, Berlin. 263–289.

Horwitz, B. A., Trad, C. H., and E. D. Lipson. 1986. Modified light-induced absorption changes in *dimY* photoresponses mutants of *Trichoderma*. *Plant Physiol.* 81:726–730.

Hubbard, R., and R. C. C. St. George. 1958. The rhodopsin system of the squid. *J. Gen. Physiol.* 41:501–528.

James, T. W., F. Crescitelli, E. R. Loew, and W. N. McFarland. 1992. The eyespot of *Euglena gracilis*: a microspectrophotometric study. *Vision Res.* 32:1583–1591.

Jennings, H. S. 1906. Behavior of the Lower Organisms. Columbia University Press, New York.

Knowles, A., and H. J. A. Dartnall. 1977. Photochemistry of extracted visual pigments. *In* The Eye, Vol. 2B, The Photobiology of Vision. H. Davson, editor. Academic Press, New York. 289–345.

Kuhlbrandt, W. 1992. Two-dimensional crystallization of membrane proteins. *Q. Rev. Biophys.* 25:1–49.

Lipson, E. D., and B. A. Horwitz. 1991. Photosensory reception and transduction. *In* Sensory Receptors and Signal Transduction. J. L. Spudich and B. H. Satir, editors. Wiley-Liss, New York. 1–64.

Lipson, E. D., and D. Presti. 1977. Light-induced absorption changes in *Phycomyces* photomutants. *Photochem. Photobiol.* 25:203–208.

Marwan, W., and D. Oesterhelt. 1990. Quantitation of photochromism of sensory rhodopsin-I by computerized tracking of *Halobacterium halobium* cells. *J. Mol. Biol.* 215:277–285.

Michel, H. 1990. General and practical aspects of membrane protein crystallization. *In* Crystallization of Membrane Proteins. H. Michel, editor. CRC Press, Boca Raton, FL. 73–89.

Muoz, V., and W. L. Butler. 1975. Photoreceptor pigment for blue light in *Neurospora crassa*. *Plant Physiol.* 55:421–426.

Neumann, R., and R. Hertel. 1994. Purification and characterization of a riboflavin-binding protein from flagella of *Euglena gracilis*. *Photochem. Photobiol.* 60:76–83.

Piccinni, E., and M. Mammi. 1978. Motor apparatus of *Euglena gracilis*: ultrastructure of the basal portion of the flagellum and the paraflagellar body. *Boll. Zool.* 45:405–414.

Poff, K. L., and W. L. Butler. 1974. Absorbance changes induced by blue light in *Phycomyces blakesleeanus* and *Dictyostelium discoideum*. *Nature.* 248:799–801.

Rosati, G., F. Verni, L. Barsanti, V. Passarelli, and P. Gualtieri. 1991. Ultrastructure of the apical zone of *Euglena gracilis*: photoreceptors and motor apparatus. *Electron Microsc. Rev.* 4:319–342.

Schlecht, P., and U. Tauber. 1975. The photochemical equilibrium in rhabdomeres of *Eledone* and its effect on dichroic absorption. *In* Photoreceptor Optics. A. W. Snyder and R. Menzel, editors. Springer-Verlag, Berlin. 316–335.

Schmidt, W., P. Galland, H. Senger, and M. Furuya. 1990. Microspecrophotometry of *Euglena gracilis*. Pterin- and flavin-like fluorescence in the paraflagellar body. *Planta.* 182:375–381.

Siebert, F. 1990. Photochromism of retinal proteins. *In* Studies of Organic Chemistry 40. Photochromism, Molecules and Systems. H. Durr and H. Bouas-Laurent, editors. Elsevier, Amsterdam. 1–34.

Sineshchekov, V. A., D. Geiß, O. A. Sineshchekov, P. Galland, and H. Senger. 1994. Fluorometric characterization of pigments associated with isolated flagella of *Euglena gracilis*: evidence or energy migration. *J. Photochem. Photobiol. B Biol.* 23:225–237.

Stavenga, D. G., R. P. Smits, and B. J. Hoenders. 1993. Simple exponential functions describing the absorbance bands of visual pigment spectra. *Vision Res.* 33:1011–1017.

Trad, C. H., B. A. Horwitz, and E. D. Lipson. 1988. Light-induced absorbance changes in extracts of *Phycomyces* sporangiophores: modifications in night-blind mutants. *J. Photochem. Photobiol.* 1:305–313.

Walne, P. L., and P. Gualtieri. 1994. Algal visual proteins: an evolutionary point of view. *Crit. Rev. Plant Sci.* 13:185–197.